

# Top quark pair production via $e^+e^-$ collision in the littlest Higgs model with T-parity at the ILC

Bingfang Yang<sup>1,2,\*</sup>, Jinzhong Han<sup>1</sup>, Lin Wang<sup>1</sup>, and Xuelei Wang<sup>1†</sup>

<sup>1</sup>*College of Physics & Information Engineering,*

*Henan Normal University, Xinxiang 453007, China*

<sup>2</sup>*Basic Teaching Department, Jiaozuo University, Jiaozuo 454000, China*

## Abstract

In the littlest Higgs model with T-parity, we studied the contributions of the new particles to the top-quark pair production via  $e^+e^-$  collision at the International Linear Collider. We calculated the top-quark pair production cross section and found this process can generate significantly relative correction. The result may be a sensitive probe of the littlest Higgs model with T-parity.

PACS numbers: 14.65.Ha,12.15.Lk,12.60.-i,13.85.Lg

---

\*Electronic address: yangbingfang@gmail.com

†Electronic address: wangxuelei@sina.com

## I. INTRODUCTION

Since the top quark was first observed at Fermilab Tevatron in 1995 [1], it is always one of the forefront topics and being studied heatedly. The top quark is the heaviest elementary fermion we have discovered and its mass is very close to the electroweak scale, so it may play an important role in the mechanism of electroweak symmetry breaking (EWSB) [2] and is considered as an ideal tool for probing new physics (NP) beyond the standard model (SM). The top-quark properties have not been precisely measured at the Tevatron due to the small statistics. But about  $10^7$  top pair signals per year will be produced at the LHC, which will be suitable to determine the top-quark properties. On the other hand, although the cross section for  $t\bar{t}$  production at the International Linear Collider(ILC) [3] is less than the LHC, the ILC will be an ideal place for further and complementary investigation of top quark compared to the complicated QCD background of the LHC as well as polarization of the initial beams.

The little Higgs theory was proposed [4] as a possible solution to the hierarchy problem and always remains a popular candidate for the NP. As a cute economical implementation of the little Higgs, the littlest Higgs (LH) model [5] is suffered from severe constraints from electroweak precision tests [6] so that the fine-tuning was reintroduced in the Higgs potential [7]. Due to the exchanges of additional heavy gauge bosons in the theories, the most serious constraints resulted from the tree-level corrections to precision electroweak observables, as well as from the small but non-vanishing vacuum expectation value (VEV) of an additional weak-triplet scalar field. In order to solve this problem, a discrete symmetry called T-parity is proposed [8], which explicitly forbids any tree-level contribution from the heavy gauge bosons to the observables involving only SM particles as external states. It also forbids the interactions that induce triplet VEV contributions. This resulting model is referred to as the littlest Higgs model with T-parity (LHT).

The LHT model predicts heavy T-odd gauge bosons which are the T-partners of the SM gauge boson and also heavy T-odd  $SU(2)$  doublet fermions. In the LHT model, the top-quark sector is quite complicated. One aspect of its phenomenology in top-quark sector is that there are interactions between the heavy fermions and the heavy gauge bosons, which can contribute to the  $Vt\bar{t}(V = \gamma, Z)$  couplings and give corrections to the  $t\bar{t}$  production cross section. In this paper, we study the LHT contributions to the relative

corrections of the top-quark pair production cross section in  $e^+e^-$  collision at the ILC. Because of this unique structure in top-quark sector, the results may be utilized to probe the LHT model.

This paper is organized as follows. In Sec.II we give a brief review of the LHT model related to our work. In Sec.III we calculate the tree and one-loop level contributions of the LHT model to the  $e^+e^- \rightarrow t\bar{t}$  and show some figures of this process in the LHT model at the ILC. Finally, we give our conclusions in Sec.IV.

## II. A BRIEF REVIEW OF THE LHT MODEL

The LHT model [8] is based on an  $SU(5)/SO(5)$  non-linear sigma model, where the global group  $SU(5)$  is spontaneously broken into  $SO(5)$  at the scale  $f \sim \mathcal{O}(TeV)$ . From the  $SU(5)/SO(5)$  breaking, there arise 14 Goldstone bosons which are described by the ‘‘pion’’ matrix  $\Pi$  as follows

$$\Pi = \begin{pmatrix} -\frac{\omega^0}{2} - \frac{\eta}{\sqrt{20}} & -\frac{\omega^+}{\sqrt{2}} & -i\frac{\pi^+}{\sqrt{2}} & -i\phi^{++} & -i\frac{\phi^+}{\sqrt{2}} \\ -\frac{\omega^-}{\sqrt{2}} & \frac{\omega^0}{2} - \frac{\eta}{\sqrt{20}} & \frac{v+h+i\pi^0}{2} & -i\frac{\phi^+}{\sqrt{2}} & \frac{-i\phi^0+\phi^P}{\sqrt{2}} \\ i\frac{\pi^-}{\sqrt{2}} & \frac{v+h-i\pi^0}{2} & \sqrt{4/5}\eta & -i\frac{\pi^+}{\sqrt{2}} & \frac{v+h+i\pi^0}{2} \\ i\phi^{--} & i\frac{\phi^-}{\sqrt{2}} & i\frac{\pi^-}{\sqrt{2}} & -\frac{\omega^0}{2} - \frac{\eta}{\sqrt{20}} & -\frac{\omega^-}{\sqrt{2}} \\ i\frac{\phi^-}{\sqrt{2}} & \frac{i\phi^0+\phi^P}{\sqrt{2}} & \frac{v+h-i\pi^0}{2} & -\frac{\omega^+}{\sqrt{2}} & \frac{\omega^0}{2} - \frac{\eta}{\sqrt{20}} \end{pmatrix} \quad (1)$$

Under T-parity the SM Higgs doublet,  $H = (-i\pi^+\sqrt{2}, (v+h+i\pi^0)/2)^T$  is T-even while other fields are T-odd.

The Goldstone bosons  $\omega^\pm, \omega^0, \eta$  are eaten by the new T-odd gauge bosons  $W_H^\pm, Z_H, A_H$  respectively, whose masses up to  $\mathcal{O}(v^2/f^2)$  are given by

$$M_{W_H} = M_{Z_H} = gf(1 - \frac{v^2}{8f^2}), M_{A_H} = \frac{g'f}{\sqrt{5}}(1 - \frac{5v^2}{8f^2}) \quad (2)$$

with  $g$  and  $g'$  being the SM  $SU(2)$  and  $U(1)$  gauge couplings, respectively.

The Goldstone bosons  $\pi^\pm, \pi^0$  are eaten by the  $W^\pm$  and  $Z$  bosons of the SM, whose masses up to  $\mathcal{O}(v^2/f^2)$  are given by

$$M_{W_L} = \frac{gv}{2}(1 - \frac{v^2}{12f^2}), M_{Z_L} = \frac{gv}{2\cos\theta_W}(1 - \frac{v^2}{12f^2}) \quad (3)$$

The photon  $A_L$  remains massless and is also T-even. Where ‘‘L’’ and ‘‘H’’ denote ‘‘light’’ and ‘‘heavy’’, respectively.

In order to preserve the T-parity, for each SM fermion, a copy of mirror fermion with T-odd quantum number is added. We denote them by  $u_H^i, d_H^i, l_H^i, \nu_H^i$ , where  $i=1, 2, 3$  are the generation index. Neglecting the  $\mathcal{O}(v^2/f^2)$  correction, the masses of the mirror fermions are given in a unified manner:

$$m_{F_H^i} = \sqrt{2}\kappa_i f \quad (4)$$

where  $\kappa_i$  are the diagonalized Yukawa couplings of the mirror fermions.

In the top sector, an additional heavy quark  $T_+$  is introduced to cancel the quadratic divergence of the Higgs mass induced by top loops. Under T-parity,  $T_+$  is even. The implementation of T-parity then requires a T-odd partner  $T_-$ . Their masses are given by

$$m_{T_+} = \frac{f}{v} \frac{m_t}{\sqrt{x_L(1-x_L)}} \left[ 1 + \frac{v^2}{f^2} \left( \frac{1}{3} - x_L(1-x_L) \right) \right] \quad (5)$$

$$m_{T_-} = \frac{f}{v} \frac{m_t}{\sqrt{x_L}} \left[ 1 + \frac{v^2}{f^2} \left( \frac{1}{3} - \frac{1}{2}x_L(1-x_L) \right) \right] \quad (6)$$

where  $x_L$  is the mixing parameter between the SM top-quark  $t$  and the new top-quark  $T_+$ .

In the LHT model, the mirror fermions open up a new flavor structure in the model. One of the important ingredients of the mirror sector is the existence of four CKM-like unitary mixing matrices, two for mirror quarks and two for mirror leptons:

$$V_{Hu}, V_{Hd}, V_{Hl}, V_{H\nu} \quad (7)$$

where  $V_{Hu}$  and  $V_{Hd}$  are for the mirror quarks,  $V_{Hl}$  and  $V_{H\nu}$  are the mirror leptons mixing matrices. These mirror mixing matrices are involved in the flavor changing interactions between the SM fermions and the mirror fermions which are mediated by the T-odd gauge bosons or T-odd Goldstone bosons. They satisfy the relation  $V_{Hu}^\dagger V_{Hd} = V_{CKM}$  and  $V_{H\nu}^\dagger V_{Hl} = V_{PMNS}$ . We follow Ref.[9] to parameterize  $V_{Hd}$  with three angles  $\theta_{12}^d, \theta_{23}^d, \theta_{13}^d$  and three phases  $\delta_{12}^d, \delta_{23}^d, \delta_{13}^d$

$$V_{Hd} = \begin{pmatrix} c_{12}^d c_{13}^d & s_{12}^d c_{13}^d e^{-i\delta_{12}^d} & s_{13}^d e^{-i\delta_{13}^d} \\ -s_{12}^d c_{23}^d e^{i\delta_{12}^d} - c_{12}^d s_{23}^d s_{13}^d e^{i(\delta_{13}^d - \delta_{23}^d)} & c_{12}^d c_{23}^d - s_{12}^d s_{23}^d s_{13}^d e^{i(\delta_{13}^d - \delta_{12}^d - \delta_{23}^d)} & s_{23}^d c_{13}^d e^{-i\delta_{23}^d} \\ s_{12}^d s_{23}^d e^{i(\delta_{12}^d + \delta_{23}^d)} - c_{12}^d c_{23}^d s_{13}^d e^{i\delta_{13}^d} & -c_{12}^d s_{23}^d e^{i\delta_{23}^d} - s_{12}^d c_{23}^d s_{13}^d e^{i(\delta_{13}^d - \delta_{12}^d)} & c_{23}^d c_{13}^d \end{pmatrix} \quad (8)$$

and follow Ref.[10] to parameterize  $V_{Hl}$  with three angles  $\theta_{12}^l, \theta_{23}^l, \theta_{13}^l$  and three phases  $\delta_{12}^l, \delta_{23}^l, \delta_{13}^l$

$$V_{Hl} = \begin{pmatrix} c_{12}^l c_{13}^l & s_{12}^l c_{13}^l e^{-i\delta_{12}^l} & s_{13}^l e^{-i\delta_{13}^l} \\ -s_{12}^l c_{23}^l e^{i\delta_{12}^l} - c_{12}^l s_{23}^l s_{13}^l e^{i(\delta_{13}^l - \delta_{23}^l)} & c_{12}^l c_{23}^l - s_{12}^l s_{23}^l s_{13}^l e^{i(\delta_{13}^l - \delta_{12}^l - \delta_{23}^l)} & s_{23}^l c_{13}^l e^{-i\delta_{23}^l} \\ s_{12}^l s_{23}^l e^{i(\delta_{12}^l + \delta_{23}^l)} - c_{12}^l c_{23}^l s_{13}^l e^{i\delta_{13}^l} & -c_{12}^l s_{23}^l e^{i\delta_{23}^l} - s_{12}^l c_{23}^l s_{13}^l e^{i(\delta_{13}^l - \delta_{12}^l)} & c_{23}^l c_{13}^l \end{pmatrix} \quad (9)$$

### III. TOP QUARK PAIR PRODUCTION VIA $e^+e^-$ COLLISION IN THE LHT MODEL

The relevant Feynman diagrams for the LHT model contributions to  $e^+e^- \rightarrow t\bar{t}$  are shown in Fig.(1-3). We can see that the Feynman diagrams consist of vertex correction, propagator correction and box diagrams. The diagrams of T-odd particles are induced by the interactions between the SM fermions and the mirror fermions mediated by the heavy T-odd gauge bosons or T-odd Goldstone bosons.

Due to the mixing between  $t$  and  $T_+$ , the  $Zt\bar{t}$  coupling is modified at tree level, which can be expressed as

$$\frac{ig}{C_W} \gamma_\mu \left[ \left( \frac{1}{2} - \frac{2}{3} S_W^2 - \frac{1}{2} x_L^2 \frac{v^2}{f^2} \right) P_L - \frac{2}{3} S_W^2 P_R \right], \quad (10)$$

where  $\theta_W$  is the Weinberg angle,  $S_W = \sin\theta_W$ ,  $C_W = \cos\theta_W$ , and  $P_L = \frac{1-\gamma_5}{2}$  and  $P_R = \frac{1+\gamma_5}{2}$  are the left-handed and right-handed projection operators, respectively. We can see that the strength of the left-handed  $Zt\bar{t}$  coupling in the LHT becomes smaller than that in the SM by the term  $-\frac{1}{2} x_L^2 \frac{v^2}{f^2}$  and the right-handed  $Zt\bar{t}$  coupling is the same as the SM.

In the NLO calculation, the high order  $\mathcal{O}(v^2/f^2)$  terms in the masses of new particles and in the Feynman rules are both neglected, the invariant amplitudes are considered to the order  $\mathcal{O}(v/f)$ . For this reason, the higher order couplings and the couplings between the scalar triplet  $\Phi$  and top quark are neglected. We can calculate the loop diagrams straightforwardly. Each loop diagram is composed of some scalar loop functions [11], which can be calculated by using LOOPTOOLS [12]. The relevant Feynman rules can be found in Ref.[13]. We use the 't Hooft-Feynman gauge, so the Goldstone bosons and the ghost fields should be involved. The analytic expressions of the amplitudes for these processes are lengthy and tedious, so we don't give the explicit expressions.

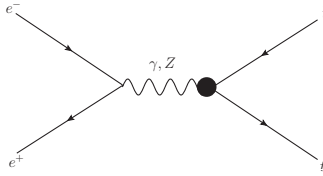
We use the dimensional regularization scheme to regulate the ultraviolet divergences and adopt the on-shell renormalization scheme to renormalize the electroweak parameters. We have checked the divergences and found the divergences of the renormalized propagator and the renormalized vertex have been canceled. There aren't divergences in the box diagrams.

The SM parameters used in our calculations are[14]

$$G_F = 1.16637 \times 10^{-5} GeV^{-2}, S_W^2 = 0.231, \alpha_e = 1/128,$$

$$M_{Z_L} = 91.2 GeV, m_t = 172.4 GeV, m_h = 120 GeV. \quad (11)$$

The relevant LHT parameters in our calculation are the scale  $f$ , the mixing parameter  $x_L$ , the mirror fermion masses and parameters in the matrices  $V_{Hu}, V_{Hd}$  and  $V_{Hl}, V_{H\nu}$ .



Where the effective vertices  $\gamma/Z t \bar{t}$  are shown in Fig.1.

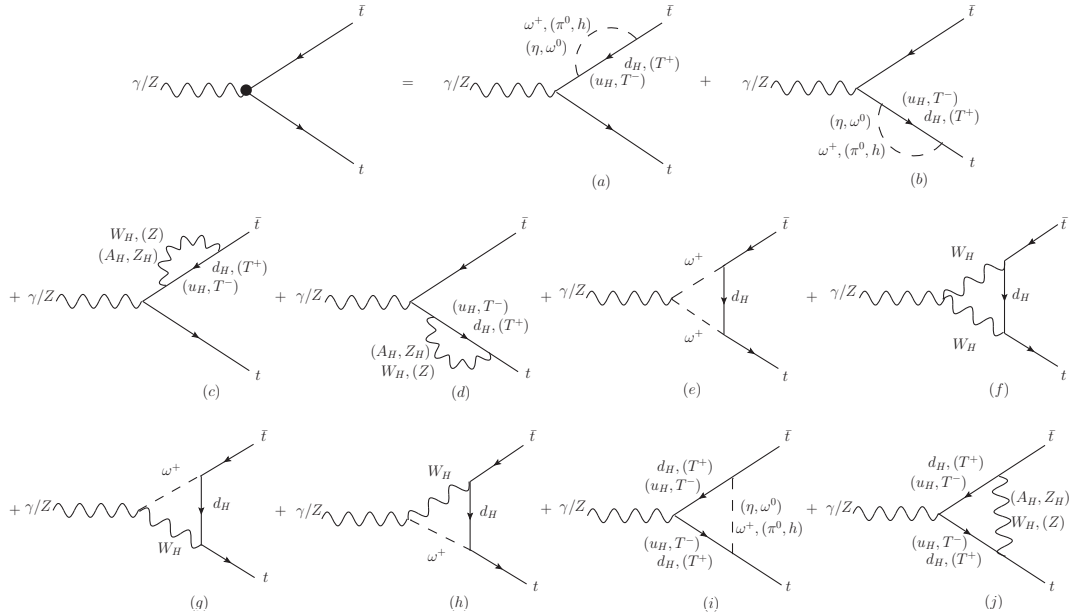


FIG. 1: Vertex correction diagrams at one-loop level in the LHT model.

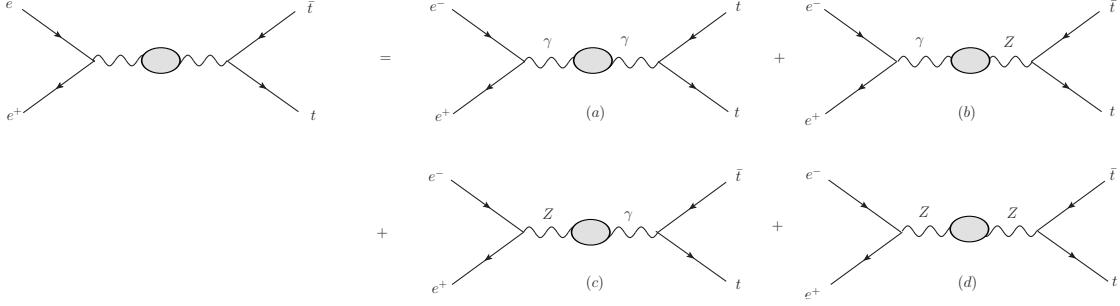


FIG. 2: Propagator correction diagrams at one-loop level in the LHT model.

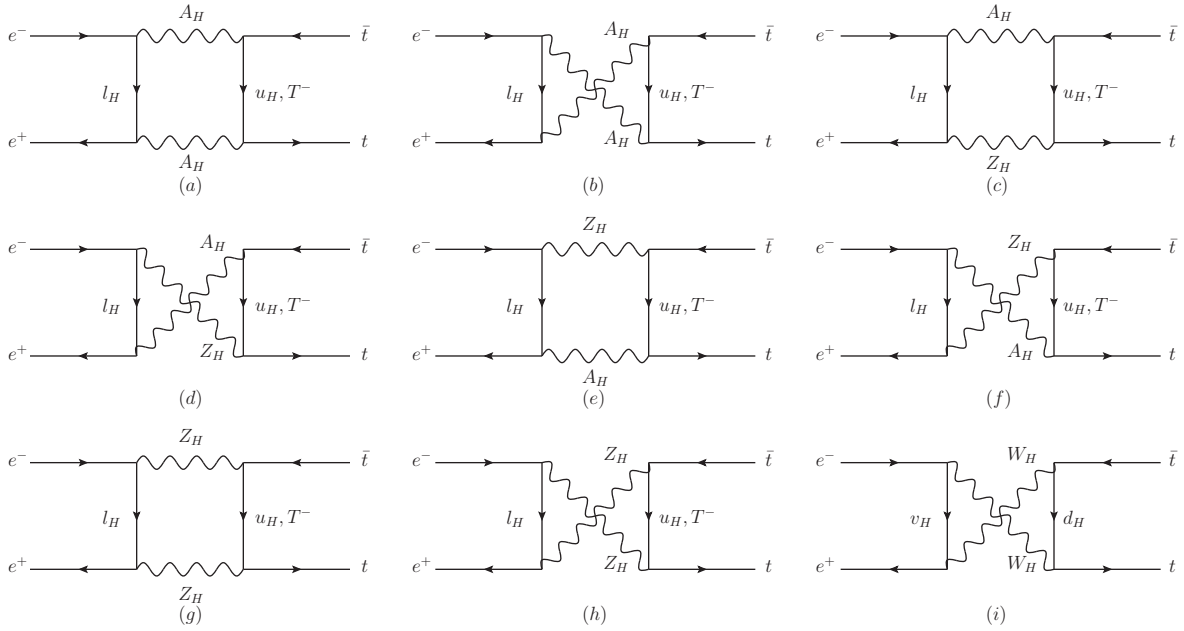


FIG. 3: Box diagrams at one-loop level in the LHT model.

For the mirror fermion masses, we get  $m_{F_H^i}$  at  $\mathcal{O}(v/f)$  and further assume

$$m_{F_H^1} = m_{F_H^2} = M_{12}, m_{F_H^3} = M_3 \quad (12)$$

For the matrices  $V_{Hu}, V_{Hd}$  and  $V_{Hl}, V_{H\nu}$ , considering the constraints in Ref.[15], we follow Ref.[16] to consider the following two scenarios:

Scenario I:  $V_{Hu} = 1, V_{Hl} = V_{CKM}$

Scenario II:  $V_{Hu} = 1, V_{Hl} = V_{PMNS}$  [17]

In Fig.4(a), we discuss the dependance of  $\delta\sigma/\sigma$  on the center-of-mass energy  $\sqrt{s}$  in

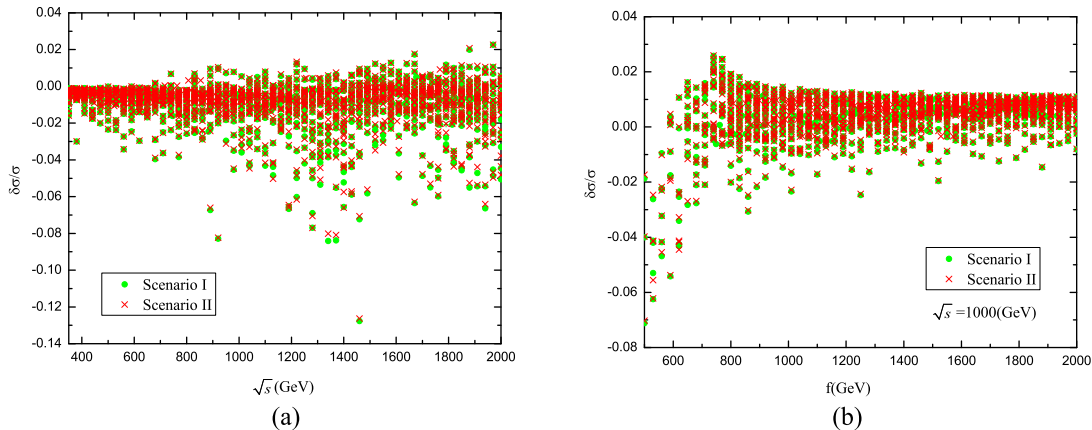


FIG. 4: The relative correction of the production cross section  $\delta\sigma/\sigma$  as functions of the center-of-mass energy  $\sqrt{s}$  (a) and the scale  $f$  (b) in two scenarios, respectively.

two scenarios. Considering the constraints of Ref.[18], we vary the parameters randomly as follows:  $M_{12} = 300 \sim 3000\text{GeV}$ ,  $M_3 = 300 \sim 3000\text{GeV}$ ,  $f = 500 \sim 2000\text{GeV}$ ,  $x_L = 0.1 \sim 0.7$ , and satisfy the relation  $m_{F_H^i} \leq 4.8f^2/\text{TeV}$ . We can see  $\delta\sigma/\sigma$  becomes larger with the  $\sqrt{s}$  increasing. When the center-of-mass energy  $\sqrt{s} \geq 600\text{GeV}$ , some peaks appear due to the threshold effects of a pair of T-odd gauge bosons  $W_H^\pm$  and the T-odd fermions. The maximum of the relative correction in two scenarios can both reach about  $-13\%$ .

In Fig.4(b), we discuss the dependance of  $\delta\sigma/\sigma$  on the scale  $f$  in two scenarios. Considering the same constraints, we vary the parameters randomly as follows:  $M_{12} = 300 \sim 3000\text{GeV}$ ,  $M_3 = 300 \sim 3000\text{GeV}$ ,  $x_L = 0.1 \sim 0.7$ , and satisfy the relation  $m_{F_H^i} \leq 4.8f^2/\text{TeV}$ . We can see  $\delta\sigma/\sigma$  tends to zero with the  $f$  increasing, which means that the correction of the LHT model decouples with the  $f$  increasing. The threshold effects of a pair of T-odd particles still exist. The maximum of the relative correction in two scenarios can both reach about  $-8\%$ .

In Fig.5, we display the transverse momentum distribution and the rapidity of the final state top quark for  $M_{12} = 600\text{GeV}$ ,  $M_3 = 1000\text{GeV}$ ,  $f = 1000\text{GeV}$ ,  $x_L = 0.4$ ,  $\sqrt{s} = 1000\text{GeV}$  in the LHT model and the SM, respectively. Because the  $d\sigma_{tot}/dP_T^t$  and the  $d\sigma_{tot}/dY_t$  change very little in two scenarios, we don't distinguish them and only show one plot as example.



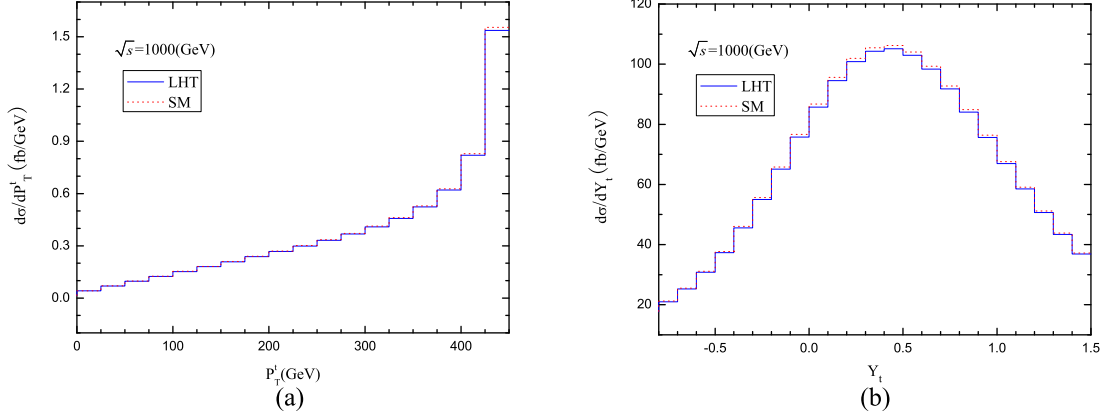


FIG. 5:  $d\sigma/dP_T^t$  as a function of the top-quark transverse momentum  $P_T^t$  (a) and  $d\sigma/dY_t$  as a function of the top-quark rapidity  $Y_t$  (b) with  $\sqrt{s} = 1000\text{GeV}$  in the SM and the LHT, respectively.

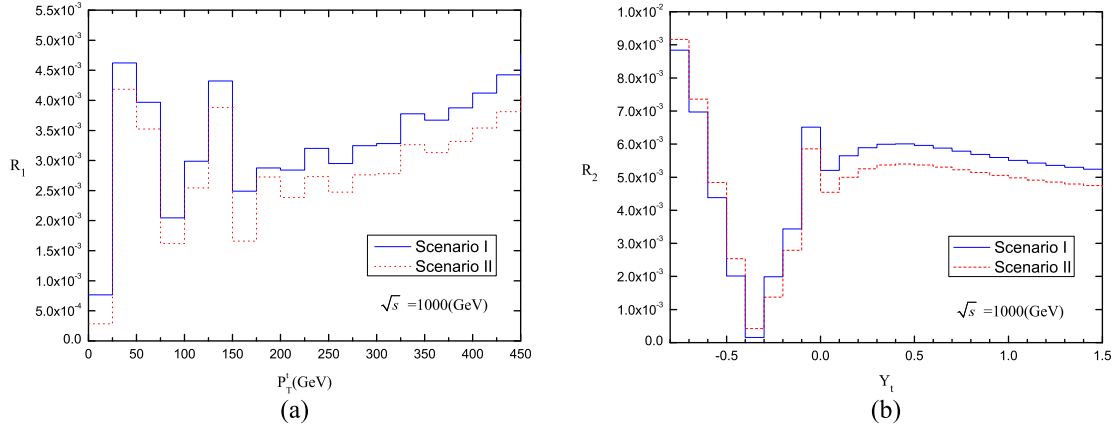


FIG. 6:  $R_1$  as a function of the top-quark transverse momentum  $P_T^t$  (a) and  $R_2$  as a function of the top-quark rapidity  $Y_t$  (b) with  $\sqrt{s} = 1000\text{GeV}$  in two scenarios, respectively.

From Fig.5(a), we can see that the transverse momentum distribution behaviour in the LHT model is similar as the SM and the values of the SM are slightly larger than the values of the LHT model. The transverse momentum values of top-quark ranging from 300 to 450  $\text{GeV}$  make the main contribution to the  $d\sigma/dP_T^t$ , which is more significant in the regions around  $P_T^t \sim 425\text{GeV}$  than in other regions.

From Fig.5(b), same as above, we can see the rapidity behaviour in the LHT model is similar as the SM and the values of the SM are slightly larger than the values of the LHT model. The rapidity values of top quark ranging from 0 to 0.9 make the main

contribution to the  $d\sigma/dY_t$ , which is more significant in the regions around  $Y_t \sim 0.4$  than in other regions. The rapidity distribution is asymmetric at the zero rapidity, which is caused by the  $Z$  boson mediated in the  $S$ -channel of the process  $e^+e^- \rightarrow t\bar{t}$ .

In Fig.6, we display the relative deviations of the transverse momentum distribution and the rapidity of the final state top quark from the SM for  $M_{12} = 600\text{GeV}, M_3 = 1000\text{GeV}, f = 1000\text{GeV}, x_L = 0.4, \sqrt{s} = 1000\text{GeV}$  in two scenarios, respectively. The relative ratio  $R_1(P_T^t)$  for the top-quark transverse momentum distribution ( $P_T^t$ ) and the relative ratio  $R_2(Y_t)$  for the top-quark rapidity ( $Y_t$ ) of the process  $e^+e^- \rightarrow t\bar{t}$  can be defined as

$$R_1 = \left| \frac{d\sigma_{tot}/dP_T^t - d\sigma_{SM}/dP_T^t}{d\sigma_{SM}/dP_T^t} \right| \quad (13)$$

$$R_2 = \left| \frac{d\sigma_{tot}/dY_t - d\sigma_{SM}/dY_t}{d\sigma_{SM}/dY_t} \right| \quad (14)$$

From Fig.6(a), we can see that is more significant in the regions around  $P_T^t \sim 25\text{GeV}, 125\text{GeV}$  and  $425\text{GeV}$  than in other regions. Furthermore, we can see  $R_1$  is larger in scenario I than in scenario II.

From Fig.6(b), we can see that is more significant in the regions around  $Y_t \sim -0.8$  than in other regions. The rapidity distribution is asymmetric at the zero rapidity, which is caused by the  $Z$  boson mediated in the  $S$ -channel of the process  $e^+e^- \rightarrow t\bar{t}$ . Different from  $R_1$ , we can see  $R_2$  is larger in scenario I when  $Y_t > -0.3$  but smaller in scenario I when  $Y_t < -0.3$ .

#### IV. CONCLUSIONS

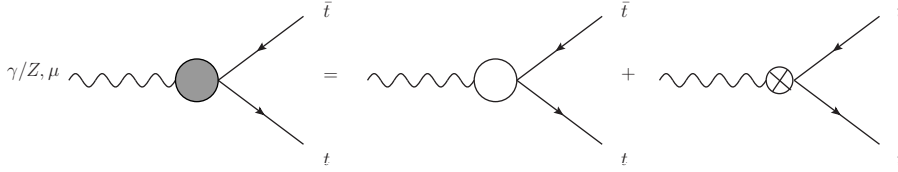
In the framework of the LHT model, we studied the one-loop contributions of the T-odd particles to the process  $e^+e^- \rightarrow t\bar{t}$  for two different scenarios. The ILC is designed with the center-of-mass energy  $\sqrt{s}=300 \sim 1500\text{GeV}$  and a precision of around 5% can be reached with  $\sqrt{s}=800 \sim 1000\text{GeV}$  and the integrated luminosity  $\mathcal{L}_{int} \simeq 1000\text{fb}^{-1}$ [19]. The relative correction of the cross section in the LHT model is significant so that the possible signals of the LHT model might be observed at the ILC. This is really interesting in testing the SM and probing the NP.

## Acknowledgments

We thank Junjie Cao for providing the calculation programs and thank Lei Wu for useful discussions and suggestions. This work is supported by the National Natural Science Foundation of China under Grant Nos.10775039, 11075045, by Specialized Research Fund for the Doctoral Program of Higher Education under Grant No.20094104110001 and by HASTIT under Grant No.2009HASTIT004.

## Appendix: The expression of the renormalization vertex $\hat{\Gamma}_{Vt\bar{t}}^\mu(V = \gamma, Z)$ and the renormalization propagator $-i\hat{\Sigma}_{\mu\nu}^{V_1V_2}$ [20]

(I)Renormalization vertex



$$\begin{aligned}\hat{\Gamma}_{\gamma t\bar{t}}^\mu &= \Gamma_{\gamma t\bar{t}}^\mu - ieQ_t\gamma^\mu(\delta Z_V^t - \gamma_5\delta Z_A^t - \frac{S_W}{2C_W}\delta Z_{ZA}) + ie\gamma^\mu(v_t - a_t\gamma_5)\frac{1}{2}\delta Z_{ZA} \\ \hat{\Gamma}_{Zt\bar{t}}^\mu &= \Gamma_{Zt\bar{t}}^\mu - ie\gamma^\mu(v_t - a_t\gamma_5)\frac{C_W}{2S_W}\delta Z_{ZA} - ieQ_t\gamma^\mu\frac{1}{2}\delta Z_{ZA} \\ &\quad + ie\gamma^\mu(v_t - a_t\gamma_5)\delta Z_V^t - ie\gamma^\mu\gamma_5(v_t - a_t\gamma_5)\delta Z_A^t\end{aligned}$$

where

$$\begin{aligned}v_t &\equiv \frac{I_t^3 - 2Q_tS_W^2}{2C_WS_W}, \quad a_t \equiv \frac{I_t^3}{2C_WS_W}, \quad I_t^3 = \frac{1}{2}, \quad Q_t = \frac{2}{3} \\ \delta Z_{ZA} &= 2\frac{\Sigma_T^{AZ}(0)}{M_{Z_L}^2} \\ \delta Z_L^t &= Re\Sigma_L^t(m_t^2) + m_t^2\frac{\partial}{\partial P_t^2}Re[\Sigma_L^t(P_t^2) + \Sigma_R^t(P_t^2) + 2\Sigma_S^t(P_t^2)]|_{P_t^2=m_t^2} \\ \delta Z_R^t &= Re\Sigma_R^t(m_t^2) + m_t^2\frac{\partial}{\partial P_t^2}Re[\Sigma_L^t(P_t^2) + \Sigma_R^t(P_t^2) + 2\Sigma_S^t(P_t^2)]|_{P_t^2=m_t^2} \\ \delta Z_V^t &= \frac{1}{2}(\delta Z_L^t + \delta Z_R^t), \quad \delta Z_A^t = \frac{1}{2}(\delta Z_L^t - \delta Z_R^t)\end{aligned}$$

$$\begin{aligned}\hat{\Gamma}_{\gamma t\bar{t}}^{LHT,\mu} &= \Gamma_{\gamma t\bar{t}}^\mu(\eta) + \Gamma_{\gamma t\bar{t}}^\mu(\omega^0) + \Gamma_{\gamma t\bar{t}}^\mu(\omega^\pm) + \Gamma_{\gamma t\bar{t}}^\mu(A_H) + \Gamma_{\gamma t\bar{t}}^\mu(Z_H) + \Gamma_{\gamma t\bar{t}}^\mu(W_H^\pm) + \Gamma_{\gamma t\bar{t}}^\mu(\omega^\pm, W_H^\pm) \\ &\quad + \delta\Gamma_{\gamma t\bar{t}}^\mu(\eta) + \delta\Gamma_{\gamma t\bar{t}}^\mu(\omega^0) + \delta\Gamma_{\gamma t\bar{t}}^\mu(\omega^\pm) + \delta\Gamma_{\gamma t\bar{t}}^\mu(A_H) + \delta\Gamma_{\gamma t\bar{t}}^\mu(Z_H) + \delta\Gamma_{\gamma t\bar{t}}^\mu(W_H^\pm) \\ \hat{\Gamma}_{Zt\bar{t}}^{LHT,\mu} &= \Gamma_{Zt\bar{t}}^\mu(\eta) + \Gamma_{Zt\bar{t}}^\mu(\omega^0) + \Gamma_{Zt\bar{t}}^\mu(\omega^\pm) + \Gamma_{Zt\bar{t}}^\mu(A_H) + \Gamma_{Zt\bar{t}}^\mu(Z_H) + \Gamma_{Zt\bar{t}}^\mu(W_H^\pm) + \Gamma_{Zt\bar{t}}^\mu(\omega^\pm, W_H^\pm) \\ &\quad + \delta\Gamma_{Zt\bar{t}}^\mu(\eta) + \delta\Gamma_{Zt\bar{t}}^\mu(\omega^0) + \delta\Gamma_{Zt\bar{t}}^\mu(\omega^\pm) + \delta\Gamma_{Zt\bar{t}}^\mu(A_H) + \delta\Gamma_{Zt\bar{t}}^\mu(Z_H) + \delta\Gamma_{Zt\bar{t}}^\mu(W_H^\pm)\end{aligned}$$

(II) Renormalization propagator

$$\text{Diagram with wavy line } V_1, \mu \text{ and } V_2, \nu \text{ and loop } = \text{Diagram with wavy line } V_1, \mu \text{ and } V_2, \nu \text{ and loop } + \text{Diagram with wavy line } V_1, \mu \text{ and } V_2, \nu \text{ and crossed loop}$$

$$-i\hat{\Sigma}_{\mu\nu}^{V_1V_2}(k) = -i\Sigma_{\mu\nu}^{V_1V_2}(k) + (-i\delta\Sigma_{\mu\nu}^{V_1V_2}(k))$$

where

$$\Sigma_{\mu\nu}^{V_1V_2}(k) = g_{\mu\nu}\Sigma_T^{V_1V_2}(k) + k_\mu k_\nu \Sigma_L^{V_1V_2}(k)$$

$$V_1, V_2 = A, Z$$

$$\delta\Sigma_{\mu\nu}^{AA}(k) = g_{\mu\nu}[\delta Z_{AA}k^2]$$

$$\delta\Sigma_{\mu\nu}^{AZ}(k) = g_{\mu\nu}\left[\frac{1}{2}(k^2 - M^2)\delta Z_{ZA} + \frac{1}{2}\delta Z_{AZ}k^2\right]$$

$$\delta\Sigma_{\mu\nu}^{ZZ}(k) = g_{\mu\nu}[-\delta M_Z^2 + (k^2 - M^2)\delta Z_{ZZ}]$$

$$\delta M_Z^2 = \text{Re}\Sigma_T^{ZZ}(M_Z^2)$$

$$\delta Z_{ZZ} = -\text{Re}\frac{\partial\Sigma_T^{ZZ}(k^2)}{\partial k^2}\Big|_{k^2=M_Z^2}, \quad \delta Z_{AZ} = -2\frac{\text{Re}\Sigma_T^{AZ}(M^2)}{M^2}$$

$$\delta Z_{ZA} = 2\frac{\Sigma_T^{AZ}(0)}{M_{Z_L}^2}, \quad \delta Z_{AA} = -\frac{\partial\Sigma_T^{AA}(k^2)}{\partial k^2}\Big|_{k^2=0}$$

$$\begin{aligned} \hat{\Sigma}_{\mu\nu}^{\gamma\gamma} &= \Sigma_{\mu\nu}^{\gamma\gamma}(f\bar{f}) + \Sigma_{\mu\nu}^{\gamma\gamma}(W_H^\pm) + \Sigma_{\mu\nu}^{\gamma\gamma}(W_H^\pm, \omega^\pm) + \Sigma_{\mu\nu}^{\gamma\gamma}(\omega^\pm) + \Sigma_{\mu\nu}^{\gamma\gamma}(u^\pm) \\ &+ \delta\Sigma_{\mu\nu}^{\gamma\gamma}(f\bar{f}) + \delta\Sigma_{\mu\nu}^{\gamma\gamma}(W_H^\pm) + \delta\Sigma_{\mu\nu}^{\gamma\gamma}(W_H^\pm, \omega^\pm) + \delta\Sigma_{\mu\nu}^{\gamma\gamma}(\omega^\pm) + \delta\Sigma_{\mu\nu}^{\gamma\gamma}(u^\pm) \\ \hat{\Sigma}_{\mu\nu}^{\gamma Z} &= \Sigma_{\mu\nu}^{\gamma Z}(f\bar{f}) + \Sigma_{\mu\nu}^{\gamma Z}(W_H^\pm) + \Sigma_{\mu\nu}^{\gamma Z}(W_H^\pm, \omega^\pm) + \Sigma_{\mu\nu}^{\gamma Z}(\omega^\pm) + \Sigma_{\mu\nu}^{\gamma Z}(u^\pm) \\ &+ \delta\Sigma_{\mu\nu}^{\gamma Z}(f\bar{f}) + \delta\Sigma_{\mu\nu}^{\gamma Z}(W_H^\pm) + \delta\Sigma_{\mu\nu}^{\gamma Z}(W_H^\pm, \omega^\pm) + \delta\Sigma_{\mu\nu}^{\gamma Z}(\omega^\pm) + \delta\Sigma_{\mu\nu}^{\gamma Z}(u^\pm) \\ \hat{\Sigma}_{\mu\nu}^{ZZ} &= \Sigma_{\mu\nu}^{ZZ}(f\bar{f}) + \Sigma_{\mu\nu}^{ZZ}(W_H^\pm) + \Sigma_{\mu\nu}^{ZZ}(W_H^\pm, \omega^\pm) + \Sigma_{\mu\nu}^{ZZ}(\omega^\pm) \\ &+ \Sigma_{\mu\nu}^{ZZ}(Z_H, \eta) + \Sigma_{\mu\nu}^{ZZ}(\omega^0, \eta) + \Sigma_{\mu\nu}^{ZZ}(\eta) + \Sigma_{\mu\nu}^{ZZ}(\omega^0) + \Sigma_{\mu\nu}^{ZZ}(u^\pm) \\ &+ \delta\Sigma_{\mu\nu}^{ZZ}(f\bar{f}) + \delta\Sigma_{\mu\nu}^{ZZ}(W_H^\pm) + \delta\Sigma_{\mu\nu}^{\gamma\gamma}(W_H^\pm, \omega^\pm) + \delta\Sigma_{\mu\nu}^{ZZ}(\omega^\pm) \\ &+ \delta\Sigma_{\mu\nu}^{ZZ}(Z_H, \eta) + \delta\Sigma_{\mu\nu}^{ZZ}(\omega^0, \eta) + \delta\Sigma_{\mu\nu}^{ZZ}(\eta) + \delta\Sigma_{\mu\nu}^{ZZ}(\omega^0) + \delta\Sigma_{\mu\nu}^{ZZ}(u^\pm) \end{aligned}$$

- 
- [1] F. Abe et al. (CDF Collaboration), Phys. Rev. Lett. 74, 2626 (1995); S. Abachi et al. (D0 Collaboration), Phys. Rev. Lett. 74, 2632 (1995).
- [2] C. T. Hill and E. H. Simmons, Phys. Rep. 381, 235 (2003).
- [3] G. Weiglein et al. [LHC/LC Study Group], Phys. Rept. 426, 47 (2006) [arXiv:hep-ph/0410364]; J. A. Aguilar-Saavedra et al. [ECFA/DESY LC Physics Working Group], arXiv:hep-ph/0106315.
- [4] N. Arkani-Hamed, A. G. Cohen, and H. Georgi, Phys. Lett. B 513, 232 (2001); N. Arkani-Hamed, et al., JHEP 0208, 020 (2002); JHEP 0208, 021 (2002); I. Low, W. Skiba, and D. Smith, Phys. Rev. D 66, 072001 (2002); D. E. Kaplan and M. Schmaltz, JHEP 0310, 039(2003).
- [5] N. Arkani-Hamed, A. G. Cohen, E. Katz, and A. E. Nelson, JHEP 0207, 034 (2002); S. Chang, JHEP 0312, 057 (2003); T. Han, H. E. Logan, B. McElrath, and L. T. Wang, Phys. Rev. D 67, 095004 (2003); M. Schmaltz and D. Tucker-smith, Ann. Rev. Nucl. Part. Sci. 55, 229 (2005).
- [6] C. Csaki, J. Hubisz, G. D. Kribs, P. Meade, J. Terning, Phys. Rev. D 67, 115002 (2003); Phys. Rev. D 68, 035009 (2003); J. L. Hewett, F. J. Petriello, and T. G. Rizzo, JHEP 0310, 062 (2003); M. C. Chen and S. Dawson, Phys. Rev. D 70, 015003 (2004); M. C. Chen, et al., Mod. Phys. Lett. A 21, 621 (2006); W. Kilian, J. Reuter, Phys. Rev. D 70, 015004 (2004).
- [7] G. Marandella, C. Schappacher and A. Strumia, Phys. Rev. D 72, 035014 (2005).
- [8] H. C. Cheng and I. Low, JHEP 0309, 051 (2003); JHEP 0408, 061 (2004); I. Low, JHEP 0410, 067 (2004); J. Hubisz and P. Meade, Phys. Rev. D 71, 035016 (2005).
- [9] M. Blanke, et al., Phys. Lett. B 646, 253 (2007).
- [10] M. Blanke, et al., JHEP 0705:013(2007).
- [11] G. 't Hooft and M. J. G. Veltman, Nucl. Phys. B 153, 365 (1979).
- [12] T. Hahn and M. Perez-Victoria, Computl. Phys. Commun. 118, 153 (1999); T. Hahn, Nucl. Phys. Proc. Suppl. 135, 333 (2004).
- [13] M. Blanke, et al., JHEP 0701, 066 (2007).
- [14] C. Amsler, et al., Phys. Lett. B 667, 1 (2008).

- [15] J.Hubisz, S. J. Lee, and G. Paz, JHEP 0606, 041 (2006); J.Hubisz, P.Meade, A.Noble, M.Perelstein,JHEP 0601:135(2006)
- [16] M.Blanke, et al.,JHEP 0705:013(2007).
- [17] Gulsheen Ahuja, Manmohan Gupta, Monika RandhawaPU Research Journal (Science) 57, 257 (2007),arXiv:hep-ph/0611324.
- [18] J.Hubisz, P.Meade, A.Noble, M.Perelstein,JHEP 0601:135(2006); Bingfang Yang, Xuelei Wang and Jinzhong Han,Nucl.Phys.B847:1-16(2011).
- [19] T. Abe et al. [American Linear Collider Group], hep-ex/0106057;  
J. A. Aguilar-Saavedra et al. [ECFA/DESY LC Physics Working Group], hep-ph/0106315;  
K. Abe et al. [ACFA Linear Collider Working Group], hep-ph/0109166;  
G. Laow et al. [ILC Technical Review Committee], second report, 2003, SLAC-R-606.
- [20] W.F.L.Hollik, Fortschr. Phys. 38: 165-260(1990); A.Denner, Fortschr. Phys.41: 307-420 (1993).